

Yeast homologues of three BLOC-1 subunits highlight KxDL proteins as conserved interactors of BLOC-1

Matthew J Hayes, Kimberley Bryon, Janani Satkurunathan and Timothy P Levine*

Address:

Department of Cell Biology, UCL Institute of Ophthalmology, Bath St, London EC1V 9EL, UK.

* To whom correspondence should be addressed.

T (+44)-20-7608-4027; F (+44)-20-7608-4034; email: tim.levine@ucl.ac.uk

Running Title: Budding yeast BLOC-1 and KxDL proteins

Key Words: endosome, endocytosis, Hermansky-Pudlak syndrome (HPS), BLOC1S1 (Blos1), cappuccino (cno), snapin, *S. cerevisiae*,

Abbreviations:

AP-3 adaptor protein complex-3; BLOC biogenesis of lysosome-related organelle complex; cno cappuccino; DUF domain of unknown function; HPS Hermansky-Pudlak syndrome; LRO lysosome-related organelle; ORF open reading frame

Abstract

BLOC-1 is one of four multi-subunit complexes implicated in sorting cargo to lysosome-related organelles, as loss of function of any of these complexes causes Hermansky-Pudlak syndrome. Eight subunits of BLOC-1 interact with each other, and with many other proteins. Identifying new interactors of BLOC-1 will increase understanding of its mechanism of action, and studies in model organisms are useful for finding such interactors. Psi-BLAST searches identify homologues in diverse model organisms, but there are significant gaps for BLOC-1, with none of its eight subunits found in *Saccharomyces cerevisiae*. Here we use more sensitive searches to identify distant homologues for three BLOC-1 subunits in *S. cerevisiae*: Blos1, snapin and cappuccino (cno). Published data on protein interactions show that in yeast these are likely to form a complex with three other proteins. One of these is the yeast homologue of the previously uncharacterized KxDL protein, which also interacts with Blos1 and cappuccino in higher eukaryotes, suggesting that KxDL proteins are key interactors with BLOC-1.

Introduction

Traffic through the secretory pathway involves the action of many multi-molecular complexes. Adaptor protein (AP-3) complexes define a traffic step from early endosomes, or in yeast from the TGN⁽¹⁾, to later endocytic compartments^(2,3). AP-3 dysfunction in humans leads to Hermansky-Pudlak Syndrome (HPS), characterized by oculocutaneous albinism and platelet dysfunction caused by defects in melanosomes and platelet dense granules respectively⁽¹⁾. These two endocytic compartments are lysosome-related organelles (LROs), a term that applies to specialized acidic organelles related to late endosomes or lysosomes^(4,5).

Biogenesis of LROs relies not only on AP-3, but also three other multimeric complexes called BLOC-1/2/3 (for biogenesis of LRO complex)⁽⁶⁾. Of these, BLOC-1 is the most complicated with eight subunits: Blos1, Blos2, Blos3 (also called BLOC1S1-3), cappuccino, dysbindin, muted, pallidin and snapin⁽⁶⁾. HPS in humans results from mutations in two of the eight BLOC-1 subunits: HPS7 and 8 arise from mutations of dysbindin and Blos3 respectively. Mutations in three other BLOC-1 subunits (pallidin, muted and cappuccino) have been identified in mouse models of HPS^(7,8). BLOC-1 has been shown to reside on endosomes^(9,10), and is required for different aspects of cargo sorting in early endosomes^(11,12). A similar function is conserved across evolution, as in flies and plants mutations in BLOC-1 subunits affect lysosome and LRO function^(13,14). A wide variety of other proteins implicated in membrane trafficking have been identified as interactors of the eight BLOC-1 subunits, mainly by yeast two-hybrid analysis⁽¹⁵⁾. Among the few interactors described to bind the intact octameric complex are AP-3 and BLOC-2⁽⁹⁾, as well as the SNAREs syntaxin-13 and SNAP-25⁽¹⁶⁾. Despite the large number of interactions known for BLOC-1, its mechanism of action is not known.

All of AP-3 and BLOC-1/2/3 are ubiquitously expressed in mammals^(4,17), suggesting that they may affect the secretory pathway in non-specialized cells. In agreement with this, HPS affects not only LROs but also the lysosome itself, such that lysosomal proteins such as CD63 are mis-routed to the cell surface⁽⁹⁾, and lipofuscin accumulates in different cell types⁽¹⁸⁾. This suggests that the mutations causing HPS might have effects in all cell types, even those lacking LROs. In the budding yeast *S. cerevisiae*, AP-3 mediates traffic of a subset of cargo to the vacuole, the terminal degradative organelle equivalent to the lysosome⁽¹⁾. Even though BLOC components are conserved widely throughout eukaryotic evolution (for example, the slime mold *Dictyostelium* has 11 of the possible 13), only two direct homologues to BLOC components have been found in any fungus: Blos1 and Blos2 in the oleaginous yeast *Yarrowia lipolytica*, but none have been identified in *S. cerevisiae*⁽¹⁹⁾.

We have extended previous iterative psi-BLAST searches, using a more sensitive technique that combines structural predictions with the detection of sequence homology. This has identified putative homologues for three BLOC-1 subunits in *S. cerevisiae*: Blos1, snapin and cno. These form a complex with three other proteins, one of which is the yeast homologue of the previously uncharacterized KxDL protein. Database mining shows that KxDL proteins have conserved interactions with BLOC-1 in higher eukaryotes.

Results and Discussion

A Blos1 homologue in *S. cerevisiae*

A psi-BLAST search seeded with human Blos1 (125 aa) identified a yeast homologue in *Y. lipolytica* (113 aa) on the second iteration, but no homologue in *S. cerevisiae* was found⁽¹⁹⁾. We reasoned that there might be a homologue of Blos1 in *S. cerevisiae* whose sequence has extensively diverged, that was missed because the set of sequences used by the iterative psi-BLAST model was too dominated by sequences closely related to human Blos1. Among the non-significant hits for Blos1 there are no *S. cerevisiae* proteins, but there are proteins from other yeast of the typical size of Blos1. For example, an ORF of 104 aa from *Kluyveromyces lactis* (a yeast that is more closely related to *Saccharomyces* than to *Yarrowia*) has an E-value = 0.09 (threshold from inclusion in psi-BLAST = 0.005, see Methods and Table S1). To test if this is a Blos1 homologue in *K. lactis*, we seeded psi-BLAST with the *K. lactis* sequence, which identified ORFs from six other yeast, including the *S. cerevisiae* ORF of unknown function YLR408Cp (122 aa). Although this psi-BLAST failed to expand, known Blos1 homologues appeared among the non-significant hits (e.g. *Rana*, E-value = 0.5; *Yarrowia*, E-value = 4, Table S1), which left open the possibility that the sequence in *K. lactis* is a Blos1 homologue, in which case YLR408Cp could also be a Blos1 homologue. To test this, we seeded a psi-BLAST search with YLR408Cp. At first this identified the same 7 yeast sequences; then the alignment expanded to include first the known fungal Blos1

homologues, then all other *Blos1* sequences (Table S1). Thus, although human *Blos1* could not detect YLR408Cp by psi-BLAST, the reverse search did establish the link, which strongly suggests that YLR408Cp is the *S. cerevisiae* homologue of *Blos1*.

We next enhanced homology detection for *Blos1* by using HHpred, which supplements sequence alignment with structure prediction⁽²⁰⁾, to achieve far greater sensitivity⁽²¹⁾. This takes advantage of the fact that proteins diverge in terms of structure much more slowly than in specific sequence, conservation of which may be undetectable. HHpred compares a structural model of the query sequence against a database of ~135,000 records that contains not only all solved structures, but also structural models of every ORF in human, fly, worm, plant and budding yeast (see Methods). HHpred searches include information not only on amino acid frequencies, but also on the position-specific probability for opening and closing gaps⁽²⁰⁾. HHpred seeded with human *Blos1* identified YLR408Cp as the sole yeast homologue (E-value 0.005, Table S2), and in the reverse search, HHpred seeded with YLR408Cp identified *Blos1* in human, fly, worm and plant (E-values 0.0001 – 0.01, Table S2). Thus, a search that includes structural information supports the psi-BLAST results that YLR408Cp is a *Blos1* homologue.

We next extended sensitivity using HHsenser, which uses an alignment originating from HHpred to find distant homologues with high sensitivity and virtual absence of false positives⁽²²⁾. HHsenser combines the iterative approach of psi-BLAST with an “intermediate profile search”, whereby information obtained from a fixed number of iterations are then used to seed new (“intermediate”) searches⁽²²⁾. In addition, HHsenser compares profiles with profiles (not with sequences), which improves sensitivity⁽²³⁾. Submitting the HHpred alignment for *Blos1* to HHsenser increased the significance of the alignment to YLR408Cp ten-fold (E-value 0.0005, Table S2). For the reverse search, HHsenser seeded with YLR408Cp produced highly significant alignments with *Blos1* in higher eukaryotes (E-values < 10⁻²⁶, Table S2). Variation in the significance of alignments depending on the initial seed is a known feature of HHsenser⁽²²⁾. These highly significant alignments strongly suggest that YLR408Cp can be assigned to be the *Blos1* homologue in *S. cerevisiae*, so we provisionally suggest the gene name BLS1, for *Blos1*-homologue, although this needs to be confirmed by functional testing for protein sorting functions.

What are the conserved features that underlie the alignment of *Blos1* with *Bls1p*? *Blos1* homologues are predicted to be helical, as is *Bls1p*. Fig 1A shows that while human *Blos1* shows great sequence homology with its plant homologue, there is only marginal sequence conservation with *Bls1p*. For all BLOC-1 subunits, short linear motifs have been identified from multiple sequence alignments, which can help identify divergent homologues⁽¹⁹⁾. In *Blos1* a conserved motif was identified at residues 87-93: “ALKEIGD” (Fig. 1B)⁽¹⁹⁾, but *Bls1p* does not contain this, and its conservation with *Blos1* is maximal in a region of 20 residues between the motif and the extreme carboxy-terminus (Fig. 1A). To analyze this conservation in *Bls1p*, previously known *Blos1* homologues were divided into two groups: animal/plant and fungal, with consensus sequences being constructed for each group (Fig. 1B). The

animal/plant *Blos1* consensus shows maximal conservation at the motif and ~20 aa on either side (44 aa in total, Fig. 1B, top row). For *Blos1* in fungi, conservation is confined to the motif and ~20aa downstream (26 residues in total, Fig. 1B, middle row). As expected from our psi-BLAST results, the sequence of *Bls1p* is closer to the fungal group than to the animal/plant group, and 13 out of 20 residues between 94-113 of *Bls1p* are shared with the fungal consensus (Fig. 1B, bottom row).

In addition to specific amino acids, key properties of the helix are conserved from human to yeast (Fig. 1C and D). Viewed as a helical wheel, both human and yeast sequences form amphipathic helices with negative charges flanking a hydrophobic face, and with positive charges and other polar residues on the opposite face (Fig. 1D). This amphipathicity correlates with conservation of hydrophobic residues at positions “a” and “d” of a heptad repeating pattern (Fig. 1C). These regions are typically not predicted to form coiled coils⁽⁸⁾, likely because most *Blos1* homologues have only one leucine in this region⁽²⁴⁾. By comparison, fungal *Blos1* homologues identified previously, as well as *Bls1p*, have 3-4 leucines here and so are predicted to form coiled-coils. The significance of this predicted difference between *Blos1* higher eukaryotes is not known. Thus, identification of *Bls1p* as a *Blos1* homologue is based on overall predicted structure, and sequence conservation with fungal *Blos1* homologues that does not include the motif identified previously.

A possible snapin homologue in *S. cerevisiae*

Continuing the search for different BLOC-1 subunits, we considered snapin (136 aa), where psi-BLAST has found homologues in metazoa, plants and protists, but not fungi⁽¹⁹⁾. HHpred seeded with snapin weakly identified the yeast ORF of unknown function YNL086Wp (102 aa, E-value 0.3, Table S2), and HHsenser improved the alignment (E-value 0.003, Table S2). In reversed searches, psi-BLAST with YNL086Wp only identified homologues in closely related yeast (Table S1). HHpred with YNL086Wp showed weak homology to snapin from human, fly and worm (E-values 0.6 – 2, Table S2), and these alignments were improved by HHsenser (E-values 0.003 – 0.09, Table S2). Even though the snapin/YNL086Wp alignment is not strong, our findings suggest that YNL086Wp could be the snapin homologue in *S. cerevisiae*, and we propose that YNL086W be named SNN1 (from snapin), again pending confirmation by functional testing.

Snapin and its known homologues have two predicted helical regions, both with predicted coiled coils, and Snn1p is highly similar, aligning without gaps across a region of 77 residues (Fig. 2A and B). Two sequence motifs were identified previously in the amino-terminal helix of snapin: “SQxEL” and “DxLaxEL” at residues 50-54 and 59-66 respectively (Fig 2A and B)⁽¹⁹⁾, the first of which is well conserved in Snn1p (Fig 2B). Other homology between snapin and Snn1p is distributed along their whole length (Fig. 2A). Within the predicted coiled-coils, key leucines in heptad repeats are conserved (Fig. 2B). Snapin and Snn1p also share the motif “RESQ” (Arg-Glu-Ser-Gln, Fig. 2B), the serine of which is phosphorylated by PKA⁽²⁵⁾. The finding that Snn1p shares functionally important sequence

elements with snapin supports the notion that it may be a snapin homologue.

A new family of cno-like proteins with a *S. cerevisiae* homologue

Psi-BLAST searches with cno (217 aa) have found homologues in mammals, fish, flies and a protist (slime mold), but not in nematode worms, plants or any fungi⁽¹⁹⁾. We hypothesized that the species lacking cno may contain homologues that have diverged beyond the ability of psi-BLAST to recognize them, but which are detectable when structural information is included in alignment searches. HHpred seeded with the protist cno (the most divergent) identified human and fly homologues with E-values < 10⁻⁵⁰. The next hits were distant matches to two proteins of unknown function (Fig. 3A): T24H7.4 in the nematode *C. elegans* (106 aa, E-value 0.2) and YDR357Cp in *S. cerevisiae* (122 aa, E-value 1), and similar results were obtained seeding HHpred with human cno (Table S2). Unlike for Bls1p/Bls1p and snapin/Snn1p, cno alignments did not improve with HHSenser. However, searches seeded with these two new sequences did yield interesting information.

For T24H7.4, psi-BLAST only found a homologue in the closely related nematode *C. briggsae*. HHpred produced weak hits to YDR357Cp, fly cno and human cno (E-values 0.6, 1 and 2 respectively, Table S2). While T24H7.4 is shorter than most cno homologues, cno in some insects is almost as short (e.g. beetle 125 aa). Therefore, we considered it possible that T24H7.4 is the missing nematode cno homologue.

Looking at YDR357Cp, psi-BLAST found a family of homologous sequences in fungi (one in each of 51 species, Table S1), but not outside fungi. HHpred with YDR357Cp (Fig. 3B) revealed weak homology both to a nematode ORF named systematically DUF2365, and to its relatives in human and fly (E-values 0.01, 0.2 and 0.4 respectively, Table S2). All that is known about the DUF2365 family (also systematically named c17orf59 from the location of the human gene) is that divergent eukaryotes have a single protein, typically of 125-325 residues, with a domain of unknown function (hence DUF) of approximately 95 residues identified by automated BLAST searches. A reciprocal HHpred search with nematode DUF2365 identified human, fly and plant DUF2365 proteins (E-value < 10⁻¹⁰); the next hit was YDR357Cp (E-value 0.006, Table S2), which strongly indicates that YDR357Cp is the yeast member of the DUF2365 family. Since YDR357C is cno-like, we propose the name CNL1. While this role has not yet been tested, there is some functional evidence that this gene functions in vacuolar protein sorting (see Conclusion).

The similarities that are shared by cno, T24H7.4, Cnl1p, and DUF2365 proteins are distributed throughout the conserved domain of approximately 95 amino acids, which is predicted to be largely helical (Fig. 3A and B). Cno is predicted to form a coiled-coil at the carboxy-terminus of its region of shared homology (Fig. 3A)⁽²⁶⁾, and the same is true for DUF2365 proteins (Fig. 3B). At the level of primary sequence, two motifs were identified in cno (Fig. 3C)⁽¹⁹⁾, but only one of these is conserved in T24H7.4 and Cnl1p (Fig. 3A and C). To visualize how elements of primary

sequence are shared between cno and fungal cno-like proteins, we made a large alignment of cno homologues and fungal cno-like sequences (Fig. S1A). This showed that there is little conservation of the first motif at residues 89-99 ("Ø-+ØØx+Ø--Ø", where Ø/-/+ are hydrophobic, acidic and basic residues respectively). In contrast, the second motif at residues 134-139 ("+Ø-+Ø±", where ± indicates charge of either type) is well conserved in fungal cno-like sequences. The alignment also revealed a third short motif ("Ø--Ø±", residues 125-129) in most fungal cno-like proteins (and all DUF2365, not shown) that is conserved to some extent in cno (Figs S1A and 3C). A tree of cno and fungal cno-like sequences shows that while they mainly divide into their two groups, there are exceptions: the cno homologue we have identified in worms (T24H7.4) and the cno homologue the choanoflagellate *Monosiga brevicollis* are intermediate between the two groups (Fig. S1B). These results support the idea that a common ancestor has diverged into the two groups of cno and cno-like proteins, the link being undetectable by conventional sequence alignment.

A yeast BLOC-1 complex that contains a KxDL protein

All BLOC-1 subunits are relatively small (between 125 and 351 residues), and are predicted to contain alpha helices⁽⁶⁾, which raises the possibility that the yeast ORFs found by HHpred are false positives, identified solely because their simple helical structure is so common. However, additional evidence that Bls1p, Snn1p and Cnl1p are BLOC-1 components comes from published data on their physical interactions. All three have been found in a single multi-subunit complex among 546 such complexes identified in a genome-wide study of protein-protein interactions in *S. cerevisiae*⁽²⁷⁾. Among the 2,400 tagged proteins purified in this study, one was Vab2p, a 31 kDa cytoplasmic protein of unknown function originally identified as a binding partner for Vac8p^(28,29), which is a peripheral vacuolar protein that co-ordinates multiple vacuolar functions^(29,30). Affinity-purified Vab2p co-precipitated five other proteins: Bls1p, Cnl1p, Snn1p, and two proteins of unknown function: YGL079Wp and YKL061Wp (Table S4)^(27,31). Precipitates of Bls1p, Cnl1p and YKL061Wp revealed five more interactions among Bls1p, Cnl1p, Snn1p, YGL079Wp and YKL061Wp (Table S4). Still more physical interactions within this group of proteins have been mapped: one affinity purification identified by its combination with similar levels of expression⁽³²⁾ and two interactions identified by two-hybrid studies⁽³³⁻³⁵⁾ (Table S4). In total, 13 of the possible 15 pair-wise interactions have been detected between the six proteins Vab2p, Bls1p, Cnl1p, Snn1p, YGL079Wp and YKL061Wp (Fig. 4A). The high density of connections suggests that they form a single complex⁽²⁷⁾. Current data do not indicate that Vab2p or any other component protein is the "node" for the complex, which will have to be determined by examining pairwise interactions in strains missing other components of the complex.

The three extra components that interact with BLOC-1 in yeast are similar to known BLOC-1 subunits in size and in predicted content of alpha-helices (with some coiled coil) but no beta-sheet (Fig. 4B). Only Vab2p has been studied previously, but apart from its interaction with Vac8p, no

function is known^(28,29). We next scanned the database for homologues of Vab2p, YGL079Wp and YKL061Wp using psi-BLAST (Table S1); no extra alignments arose from HHpred. Homologues for Vab2p were found in fungi only. For YKL061Wp, homologues were restricted to close relatives of *S. cerevisiae* (Table S1). Since the majority of physical interactions documented for YKL061W are with BLOC-1 subunits^(27,31,33-35), we propose the name BLI1, for BLOC-1 interactor.

Unlike Vab2p and Bli1p, YGL079Wp is in a conserved protein family, with a single identifiable member in most eukaryotes, from mammals to plants (Table S1). However, none of the homologues have been characterized. Automated database curation has designated them as IPR019371, Pfam10241, or DUF-KxDL. They are all short proteins, defined by a conserved helical region of 90 residues that includes a "KxDL" (Lys-x-Asp-Leu) motif near the carboxy-terminus (Fig. 4B). Since YGL079W is the yeast KxDL homologue, we propose the name KXD1.

The multiple interactions between all of Bli1p, Snn1p, Cnl1p, Vab2p, Bli1p and Kxd1p indicate that the latter three might also be subunits of BLOC-1 in yeast. In support of this, high-throughput analysis of localization ascribes all six ORFs to a punctate distribution, in some cases reported to co-localize with endosomes⁽³⁶⁾.

Conclusions

Including structural information in homology searches identified potential yeast homologues for Blos1 and snapin, and a cno-like protein. The same approach found no homologues in yeast for the five remaining BLOC-1 subunits (Blos2, Blos3, muted, dysbindin, and pallidin), but did identify a new homologue of muted in *C. elegans* (C34D4.13, not shown). This indicates that whatever the function may be of the yeast complex we have highlighted, it may be only distantly related to BLOC-1 in mammals. Nevertheless, there is some evidence that the yeast proteins are performing a function that parallels BLOC-1 in mammals, since a genome-wide screen that identified ~200 genes functioning in vacuolar protein sorting included both CNL1 and KXD1, as well as all four sub-units of AP-3, but none of AP-1,-2 and clathrin⁽³⁷⁾. The inclusion of Kxd1p in complexes containing yeast BLOC-1 homologues is particularly significant because, although KxDL proteins are completely uncharacterized, in higher eukaryotes they recapitulate some of the interactions with BLOC-1 subunits (Fig. 4): in *D. melanogaster* and *C. elegans*, the KxDL protein interacts with Blos1⁽³⁸⁾; in *C. elegans*, the KxDL protein interacts both with the newly discovered cno (T24H7.4), and with the DUF2365 homologue⁽³⁹⁾. Conservation of interactions in yeast, worms and flies suggests that KxDL proteins may be key interactors with BLOC-1 in mammals.

Although it has not been shown that any of the interactions of the yeast complex occur simultaneously, the density of interactions among the six subunits is predicted to generate a multimeric complex⁽²⁷⁾. Would this be similar to BLOC-1 in higher eukaryotes, which, by a combination of size exclusion chromatography and velocity sedimentation, has been estimated to be an asymmetric complex of 200 kDa

⁽⁴⁰⁾? For most of the eight subunits, a large proportion co-migrates and co-precipitates in these large complexes^(8,26,41). However purification of the complex has not yet been achieved, so its complete composition is not known. Our results predict that BLOC-1 might include KxDL or DUF2365 proteins. Knowing conserved components and interactions in yeast, it will now be possible to study ancestral functions of BLOC-1 in a genetically tractable model organism.

Methods

Psi-BLAST: The psi-BLAST tool examining the non-redundant protein database at NCBI. E-values returned here (and by other tools, below) give the average number of false positives expected to randomly produce an alignment as good as this. An E-value of 10 means that 10 wrong hits are expected to occur with the extent of alignment observed, while numbers very much smaller than one indicate likely significance. We used a threshold E-value of 0.005 for inclusion of alignments from one iteration of psi-BLAST in the next iteration. Also searches were limited to eukaryotes, and sequences masked for the lookup table only. Psi-BLAST was iterated until new sequences added to the list were larger proteins including other domains of known function. Sequences from transcripts with frame shift errors were excluded.

HHpred: The HHpred tool⁽²⁰⁾, which is part of the MPI bioinformatics toolkit (<http://toolkit.tuebingen.mpg.de>), was used to search against the protein databank of structures clustered at 70% sequence identity (PDB70), and to examine the genomes of five phylogenetically diverse organisms: *H. sapiens*, *D. melanogaster*, *C. elegans*, *A. thaliana*, and *S. cerevisiae*, with a total of ~135,000 records in total. Alignments were carried out with default settings in the local mode. E-values returned by HHpred and reported here are based on sequence alone, excluding secondary structural similarity, so hits can be significant even when the E-value is ~ 1⁽²⁰⁾. Some HHpred alignments were submitted to HHSenser, using default settings⁽²²⁾. Coiled-coils were analyzed at www.ch.embnet.org/ using default settings; positions where any of the three windows scores ≥ 0.5 were considered positive. Structural predictions were made by Psi-Pred 3.0. Consensus sequences for Blos1 and snapin were made by Multiple Sequence Comparison by Log-Expectation (MUSCLE) at EBI. For each position in the consensus, conservation was scored by comparison to maximum consensus strength: <50% weak, 50-75% moderate, and $\geq 75\%$ high. The alignment for Fig. S1 was made by Kalign at EBI, and coloured with the Clustalx scheme.

Acknowledgements

Funding: Wellcome Trust (grant #082119).

References

1. Odorizzi G, Cowles CR, and Emr SD. The AP-3 complex: a coat of many colours. Trends Cell Biol 1998; 8:282-288.

2. Peden AA, Oorschot V, Hesser BA, Austin CD, Scheller RH, and Klumperman J. Localization of the AP-3 adaptor complex defines a novel endosomal exit site for lysosomal membrane proteins. *J Cell Biol* 2004; 164:1065-1076.
3. Theos AC, Tenza D, Martina JA, Hurbain I, Peden AA, Sviderskaya EV, Stewart A, Robinson MS, Bennett DC, Cutler DF, Bonifacino JS, Marks MS, and Raposo G. Functions of adaptor protein (AP)-3 and AP-1 in tyrosinase sorting from endosomes to melanosomes. *Mol Biol Cell* 2005; 16:5356-5372.
4. Bonifacino JS. Insights into the biogenesis of lysosome-related organelles from the study of the Hermansky-Pudlak syndrome. *Ann N Y Acad Sci* 2004; 1038:103-114.
5. Raposo G, Marks MS, and Cutler DF. Lysosome-related organelles: driving post-Golgi compartments into specialisation. *Curr Opin Cell Biol* 2007; 19:394-401.
6. Dell'Angelica EC. The building BLOC(k)s of lysosomes and related organelles. *Curr Opin Cell Biol* 2004; 16:458-464.
7. Falcon-Perez JM and Dell'Angelica EC. The pallidin (Pldn) gene and the role of SNARE proteins in melanosome biogenesis. *Pigment Cell Res* 2002; 15:82-86.
8. Starcevic M and Dell'Angelica EC. Identification of snapin and three novel proteins (BLOS1, BLOS2, and BLOS3/reduced pigmentation) as subunits of biogenesis of lysosome-related organelles complex-1 (BLOC-1). *J Biol Chem* 2004; 279:28393-28401.
9. Di Pietro SM, Falcon-Perez JM, Tenza D, Setty SR, Marks MS, Raposo G, and Dell'Angelica EC. BLOC-1 interacts with BLOC-2 and the AP-3 complex to facilitate protein trafficking on endosomes. *Mol Biol Cell* 2006; 17:4027-4038.
10. Salazar G, Craige B, Styers ML, Newell-Litwa KA, Doucette MM, Wainer BH, Falcon-Perez JM, Dell'Angelica EC, Peden AA, Werner E, and Faundez V. BLOC-1 complex deficiency alters the targeting of adaptor protein complex-3 cargoes. *Mol Biol Cell* 2006; 17:4014-4026.
11. Setty SR, Tenza D, Truschel ST, Chou E, Sviderskaya EV, Theos AC, Lamoreux ML, Di Pietro SM, Starcevic M, Bennett DC, Dell'Angelica EC, Raposo G, and Marks MS. BLOC-1 is required for cargo-specific sorting from vacuolar early endosomes toward lysosome-related organelles. *Mol Biol Cell* 2007; 18:768-780.
12. Newell-Litwa K, Salazar G, Smith Y, and Faundez V. Roles of BLOC-1 and adaptor protein-3 complexes in cargo sorting to synaptic vesicles. *Mol Biol Cell* 2009; 20:1441-1453.
13. Cheli VT, Daniels RW, Godoy R, Hoyle DJ, Kandachar V, Starcevic M, Martinez-Agosto JA, Poole S, DiAntonio A, Lloyd VK, Chang HC, Krantz DE, and Dell'Angelica EC. Genetic modifiers of abnormal organelle biogenesis in a *Drosophila* model of BLOC-1 deficiency. *Hum Mol Genet* 2010; 19:861-878.
14. Cui Y, Li X, Chen Q, He X, Yang Q, Zhang A, Yu X, Chen H, Liu N, Xie Q, Yang W, Zuo J, Palme K, and Li W. BLOS1, a putative BLOC-1 subunit, interacts with SNX1 and modulates root growth in *Arabidopsis*. *J Cell Sci* 2010; 123:3727-3733.
15. Rodriguez-Fernandez IA and Dell'Angelica EC. A data-mining approach to rank candidate protein-binding partners-The case of biogenesis of lysosome-related organelles complex-1 (BLOC-1). *J Inher Metab Dis* 2009; 32:190-203.
16. Ghiani CA, Starcevic M, Rodriguez-Fernandez IA, Nazarian R, Cheli VT, Chan LN, Malvar JS, de Vellis J, Sabatti C, and Dell'Angelica EC. The dysbindin-containing complex (BLOC-1) in brain: developmental regulation, interaction with SNARE proteins and role in neurite outgrowth. *Mol Psychiatry* 2010; 15:204-215.
17. Dell'Angelica EC, Ohno H, Ooi CE, Rabinovich E, Roche KW, and Bonifacino JS. AP-3: an adaptor-like protein complex with ubiquitous expression. *Embo J* 1997; 16:917-928.
18. Shotelersuk V and Gahl WA. Hermansky-Pudlak syndrome: models for intracellular vesicle formation. *Mol Genet Metab* 1998; 65:85-96.
19. Cheli VT and Dell'Angelica EC. Early origin of genes encoding subunits of biogenesis of lysosome-related organelles complex-1, -2 and -3. *Traffic* 2010; 11:579-586.
20. Soding J, Biegert A, and Lupas AN. The HHpred interactive server for protein homology detection and structure prediction. *Nucleic Acids Res* 2005; 33:W244-248.
21. Battey JN, Kopp J, Bordoli L, Read RJ, Clarke ND, and Schwede T. Automated server predictions in CASP7. *Proteins* 2007; 69 Suppl 8:68-82.
22. Soding J, Remmert M, Biegert A, and Lupas AN. HHSenser: exhaustive transitive profile search using HMM-HMM comparison. *Nucleic Acids Res* 2006; 34:W374-378.
23. Pietrokovski S. Searching databases of conserved sequence regions by aligning protein multiple-alignments. *Nucleic Acids Res* 1996; 24:3836-3845.
24. Moitra J, Szilak L, Krylov D, and Vinson C. Leucine is the most stabilizing aliphatic amino acid in the d position of a dimeric leucine zipper coiled coil. *Biochemistry* 1997; 36:12567-12573.
25. Chheda MG, Ashery U, Thakur P, Rettig J, and Sheng ZH. Phosphorylation of Snapin by PKA modulates its interaction with the SNARE complex. *Nat Cell Biol* 2001; 3:331-338.
26. Ciciotte SL, Gwynn B, Moriyama K, Huizing M, Gahl WA, Bonifacino JS, and Peters LL. Cappuccino, a mouse model of Hermansky-Pudlak syndrome, encodes a novel protein that is part of the pallidin-muted complex (BLOC-1). *Blood* 2003; 101:4402-4407.
27. Krogan NJ, Cagney G, Yu H, Zhong G, Guo X, Ignatchenko A, Li J, Pu S, Datta N, Tikuisis AP, Punna T, Peregrin-Alvarez JM, Shales M, Zhang X, Davey M, et al. Global landscape of protein complexes in the yeast *Saccharomyces cerevisiae*. *Nature* 2006; 440:637-643.
28. Pan X, Roberts P, Chen Y, Kvam E, Shulga N, Huang K, Lemmon S, and Goldfarb DS. Nucleus-vacuole junctions in *Saccharomyces cerevisiae* are formed

- through the direct interaction of Vac8p with Nvj1p. *Mol Biol Cell* 2000; 11:2445-2457.
29. Tang F, Peng Y, Nau JJ, Kauffman EJ, and Weisman LS. Vac8p, an armadillo repeat protein, coordinates vacuole inheritance with multiple vacuolar processes. *Traffic* 2006; 7:1368-1377.
 30. Wang YX, Catlett NL, and Weisman LS. Vac8p, a vacuolar protein with armadillo repeats, functions in both vacuole inheritance and protein targeting from the cytoplasm to vacuole. *J Cell Biol* 1998; 140:1063-1074.
 31. Collins SR, Kemmeren P, Zhao XC, Greenblatt JF, Spencer F, Holstege FC, Weissman JS, and Krogan NJ. Toward a comprehensive atlas of the physical interactome of *Saccharomyces cerevisiae*. *Mol Cell Proteomics* 2007; 6:439-450.
 32. Chin CH, Chen SH, Ho CW, Ko MT, and Lin CY. A hub-attachment based method to detect functional modules from confidence-scored protein interactions and expression profiles. *BMC Bioinformatics* 2010; 11 Suppl 1:S25.
 33. Uetz P, Giot L, Cagney G, Mansfield TA, Judson RS, Knight JR, Lockshon D, Narayan V, Srinivasan M, Pochart P, Qureshi-Emili A, Li Y, Godwin B, Conover D, Kalbfleisch T, et al. A comprehensive analysis of protein-protein interactions in *Saccharomyces cerevisiae*. *Nature* 2000; 403:623-627.
 34. Ito T, Chiba T, Ozawa R, Yoshida M, Hattori M, and Sakaki Y. A comprehensive two-hybrid analysis to explore the yeast protein interactome. *Proc Natl Acad Sci U S A* 2001; 98:4569-4574.
 35. Yu H, Braun P, Yildirim MA, Lemmens I, Venkatesan K, Sahalie J, Hirozane-Kishikawa T, Gebreab F, Li N, Simonis N, Hao T, Rual JF, Dricot A, Vazquez A, Murray RR, et al. High-quality binary protein interaction map of the yeast interactome network. *Science* 2008; 322:104-110.
 36. Huh WK, Falvo JV, Gerke LC, Carroll AS, Howson RW, Weissman JS, and O'Shea EK. Global analysis of protein localization in budding yeast. *Nature* 2003; 425:686-691.
 37. Norambuena L, Zouhar J, Hicks GR, and Raikhel NV. Identification of cellular pathways affected by Sortin2, a synthetic compound that affects protein targeting to the vacuole in *Saccharomyces cerevisiae*. *BMC Chem Biol* 2008; 8:1.
 38. Giot L, Bader JS, Brouwer C, Chaudhuri A, Kuang B, Li Y, Hao YL, Ooi CE, Godwin B, Vitols E, Vijayadamodar G, Pochart P, Machineni H, Welsh M, Kong Y, et al. A protein interaction map of *Drosophila melanogaster*. *Science* 2003; 302:1727-1736.
 39. Simonis N, Rual JF, Carvunis AR, Tasan M, Lemmens I, Hirozane-Kishikawa T, Hao T, Sahalie JM, Venkatesan K, Gebreab F, Cevik S, Klitgord N, Fan C, Braun P, Li N, et al. Empirically controlled mapping of the *Caenorhabditis elegans* protein-protein interactome network. *Nat Methods* 2009; 6:47-54.
 40. Falcon-Perez JM, Starcevic M, Gautam R, and Dell'Angelica EC. BLOC-1, a novel complex containing the pallidin and muted proteins involved in the biogenesis of melanosomes and platelet-dense granules. *J Biol Chem* 2002; 277:28191-28199.
 41. Li W, Zhang Q, Oiso N, Novak EK, Gautam R, O'Brien EP, Tinsley CL, Blake DJ, Spritz RA, Copeland NG, Jenkins NA, Amato D, Roe BA, Starcevic M, Dell'Angelica EC, et al. Hermansky-Pudlak syndrome type 7 (HPS-7) results from mutant dysbindin, a member of the biogenesis of lysosome-related organelles complex 1 (BLOC-1). *Nat Genet* 2003; 35:84-89.

Figure Legends

Fig. 1. Alignment of *Blos1* homologues with *Bls1p*.

A. Secondary structural prediction for *Blos1* homologues.

Blos1 in *H. sapiens* (*Hs*) was aligned by HHpred with *Blos1* in *Arabidopsis thaliana* (*At*) and *Bls1p* in *S. cerevisiae* (*Sc*). Cylinders represent alpha helices (no beta sheet predicted). Alignments are from HHSenser seeded with the human sequence, with asterisks indicating gaps of single residues, and conservation indicated by | : and · (excellent, good & moderate respectively). Black dots above indicated the motif at residues 87–93 of human *Blos1* identified previously⁽¹⁹⁾. White dots indicate residues 94–113 of *Bls1p*/YLR408Cp, the region that is most highly shared by *Bls1p* and fungal sequences (see B).

B. Alignment of the carboxy-terminal half of *Bls1p* with consensus sequences from known *Blos1* homologues.

The top two rows are consensus sequences created using MUSCLE (see Methods) from 62 previously identified *Blos1* sequences, 35 from animals and plants, and 27 from fungi (see Table S3). All positions in these consensus sequences were scored as weakly, moderately or highly conserved (see Methods). The regions shown are those that are rich in highly conserved residues (indicated in upper case and bold). For animal/plant *Blos1* (top row) the region is equivalent to residues 70–113 of human *Blos1* (44 residues). For fungal *Blos1* (middle row) the region is equivalent to residues 88-113 (26 residues). Conserved hydrophobicity is indicated by Ø. Residue colours are: basic – blue, acidic – red, hydrophobic – yellow on black, alanine – grey on black. The bottom row is the homologous region from *Bls1p* (residues 69–113). Here residues that are shared with either of the consensus sequences above are indicated by bold capitals and with asterisks. White dots above the sequence indicate the region of maximum identity between *Bls1p* (residues 94–113) and the fungal consensus. As in A, the motif described by Cheli *et al.*⁽¹⁹⁾ is indicated by black dots.

C. Alignment of the most conserved regions of six key *Blos1* homologues.

Alignment of *Blos1* sequences from human (*Hs*), fly (*Dm*), worm (*Ce*), plant (*At*), oleaginous yeast (*Yl*) and budding yeast (*Sc*) covering the conserved 27 residues indicated by black and white dots as in (B). Residue colours are as in (A). Heptad repeats with hydrophobic residues at positions “a” and “d” are shown below, together with the degree of conservation at each position as calculated by MUSCLE: excellent, good or moderate (indicated by | : and ·).

D. Helical wheel projections of 20 residues from *Blos1* and *Bls1p*.

Helical wheel projections for carboxy-terminal

helices of human Blos1 and Bli1p (residues 94–113 for both). Circle colours: basic – blue, acidic – red, hydrophobic – yellow, alanine – grey, serine/threonine – purple, hydrophilic – pink.

Fig. 2. Alignment of snapin homologues with Snn1p.

A. Secondary structural prediction for Snapin homologues. Human snapin was aligned with the plant homologue and with Snn1p, as in Fig. 1A. Motifs identified by Cheli *et al.* are indicated by black dots. Predicted coiled-coils are shown, with those near the amino-terminus of Snn1p in grey to indicate their prediction strength is just below the threshold of 0.5 (0.43).

B. Alignment of the central region of 77 amino acids from five key snapin homologues. Sequences from the central region (as indicated by the dotted lines) of snapin homologues from human (*Hs*: 33-109), fly (*Dm*: 34-110), worm (*Ce*: 21-96), plant (*At*: 45-120), and budding yeast (*Sc*: 24-100) were aligned, residue colours as in Fig 1B. Below is a consensus sequence made from 38 snapin homologues (see Table S3), with conserved hydrophobicity indicated by “Ø”, conserved K or R indicated by “+”, and the most conserved positions shown in capitals and bold. The bottom line shows heptad repeats with hydrophobic residues at positions “a” and “d”. In each of the two helices, one of the key “a” or “d” positions is not hydrophobic (shown as white “a” or “d” on black). Leucine is common at positions “a” and “d” (56%), explaining why these helices are predicted to form coiled-coils⁽²⁴⁾. Boxed “RESQ” above indicates the PKA phosphorylation site found in both human snapin and Snn1p. Black dots above are previously identified motifs, as in A.

Fig. 3. Alignment of cno and newly described homologues

A and B. Secondary structural prediction and alignment of cno and sequences identified by HHpred. Alignments of (A) Cno from human with T24H7.4 from *C. elegans* (*Ce*) and Cnl1p in *S. cerevisiae* (*Sc*); and (B) Cnl1p with DUF2365 proteins in *C. elegans* and human. Alignments shown as in Fig. 1A, but requiring gaps as indicated. Predicted helices and coiled-coils are indicated as in Fig. 2A. Black dots above indicate motifs identified by Cheli *et al.*⁽¹⁹⁾ in cno. White dots above indicate a motif we identify to be shared between cno and Cnl1 sequences - see Fig. S1 and (C).

C. Alignment of the central region from cno homologues and cno-like homologues in fungi. The central region of cno in human (*Hs*: 61-159) was aligned to the homologous region from cno in zebrafish (*Dr*: 84-180), cno in fly (*Dm*: 5-102), T24H7.4 in worm (*Ce*: 14-103), and the cno-like proteins in the filamentous fungus *Neurospora* (*Nc*: 70-161), budding yeast (*Sc*: 21-114), and the oleaginous yeast *Yarrowia* (*Yl*: 21-113); residue colours as in Fig 1B. Dots above represent motifs (see text and Fig. S1). Below is a consensus sequence made from these seven sequences. Here and in the motifs above the alignment, conserved residues are: “Ø” = hydrophobic, “+” = K/R, “-” = D/E, “±” = K/R/D/E. Lower case “ø” indicates where hydrophobicity is weakly conserved. The bottom line shows heptad repeats underlying predicted coiled-coils at the carboxy-terminus, with hydrophobic residues at positions “a” and “d” (except for one “d” position shown as white “d” on black). Leucine is common at positions “a” and “d” (31%), explaining why these helices are predicted to form coiled-coils⁽²⁴⁾.

Fig 4. A complex of six yeast proteins includes all three BLOC-1 subunits.

A. Known direct physical interactions between six proteins identified in Vab2p complexes. Black and grey lines represent interactions defined by affinity purification/mass spectrometry and yeast two hybrid, respectively. The Vab2p-Bli1p and Kxd1p-Snn1p interactions are indicated by dashed lines as they scored below the threshold defining core interactions (Table S4). Interactions obtained in two or three studies are indicated by correspondingly thicker lines. Of the possible 15 pair-wise interactions^(27,32), 11 were found by direct interaction^(27,32), and two by two hybrid. Asterisks indicate two interactions of KxDL proteins that are recapitulated in higher eukaryotes (see Conclusion).

B. Predicted secondary structure of three yeast proteins interacting with BLOC-1. The predicted helical nature of Vab2p, Bli1p and Kxd1p is shown, together with regions predicted to form coiled coils, as in Fig. 2A. The conserved KxDL motif at residues 175-8 of Kxd1p is indicated.

Figure 1

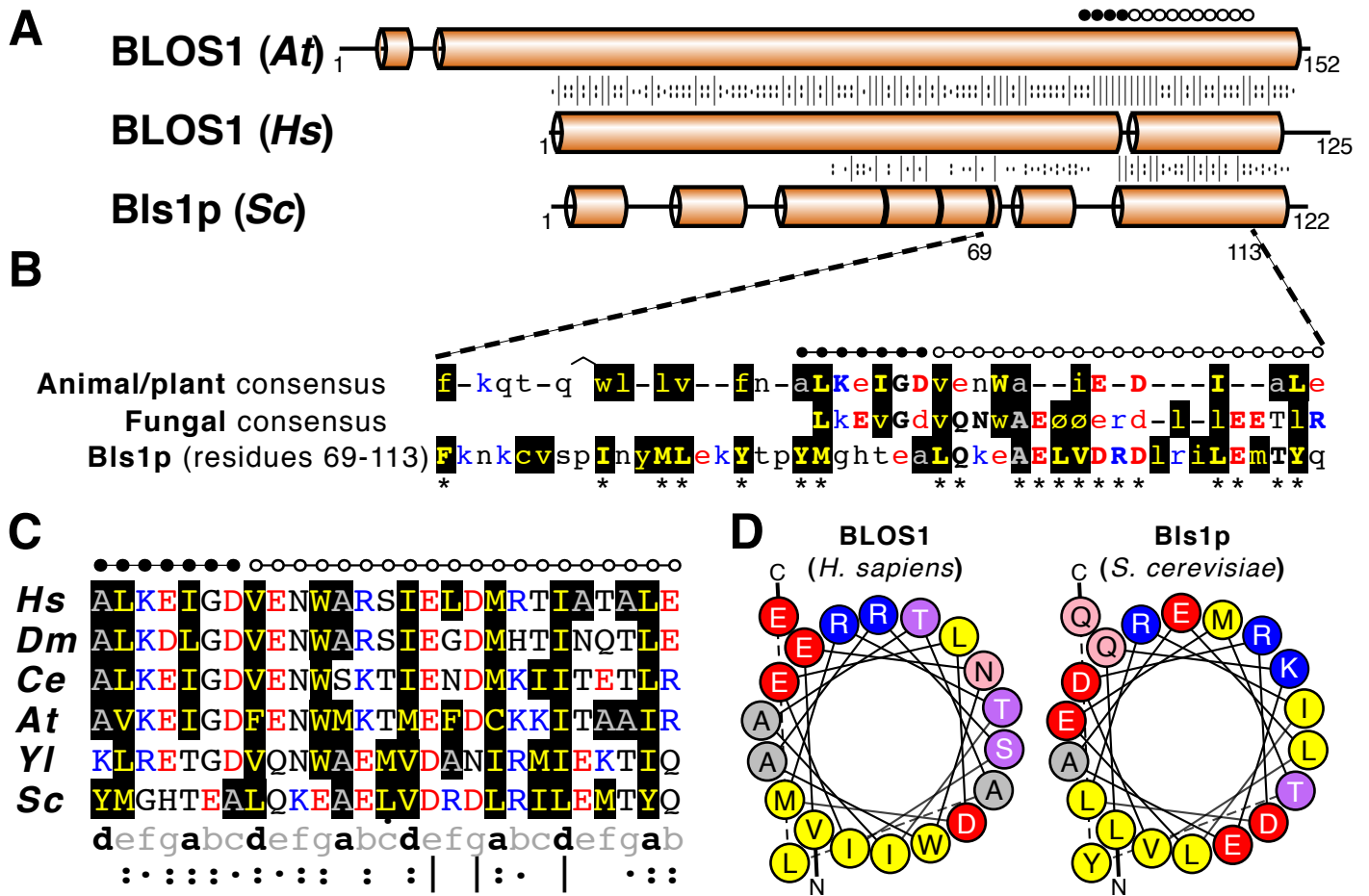


Figure 2

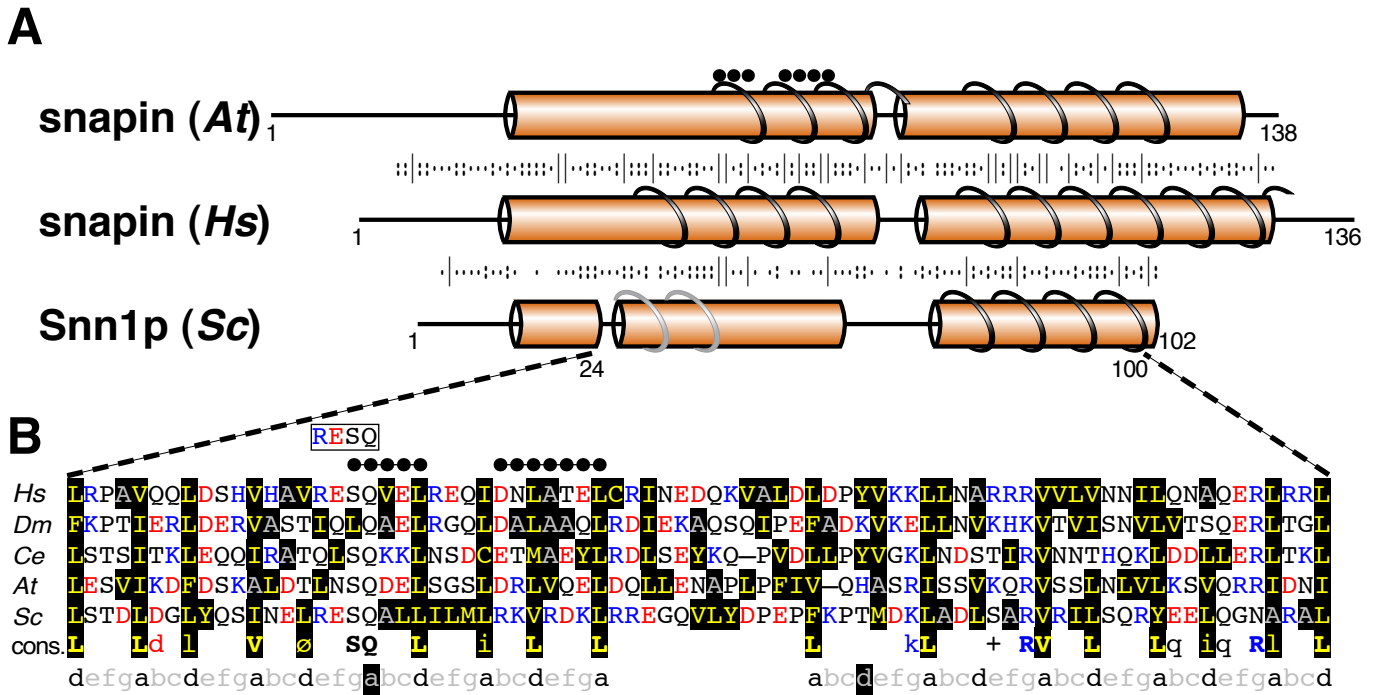
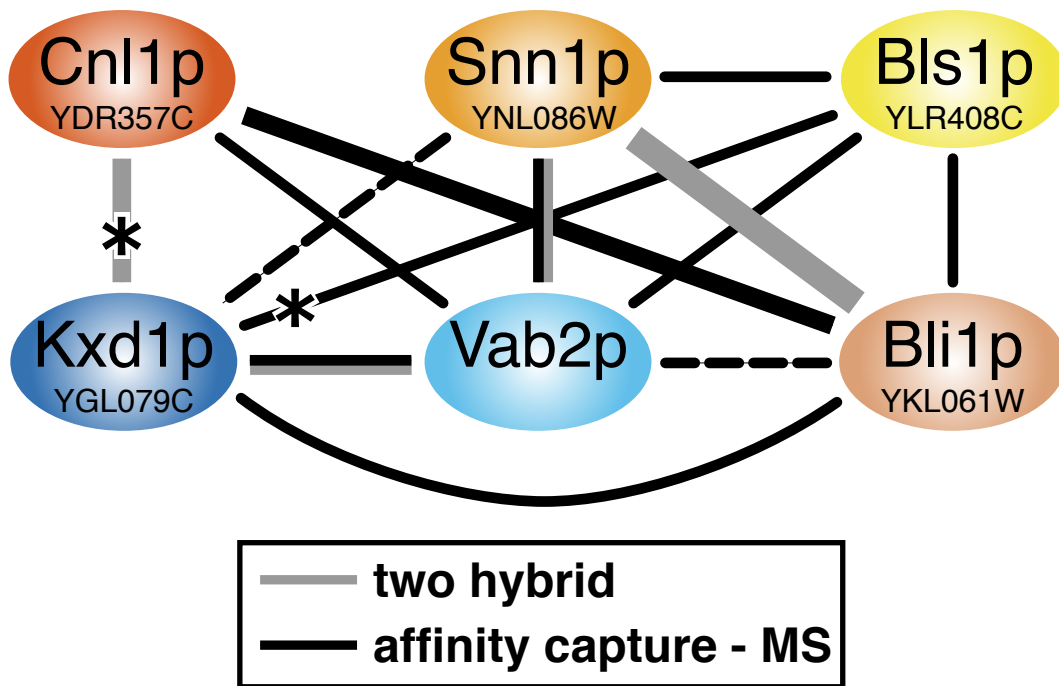
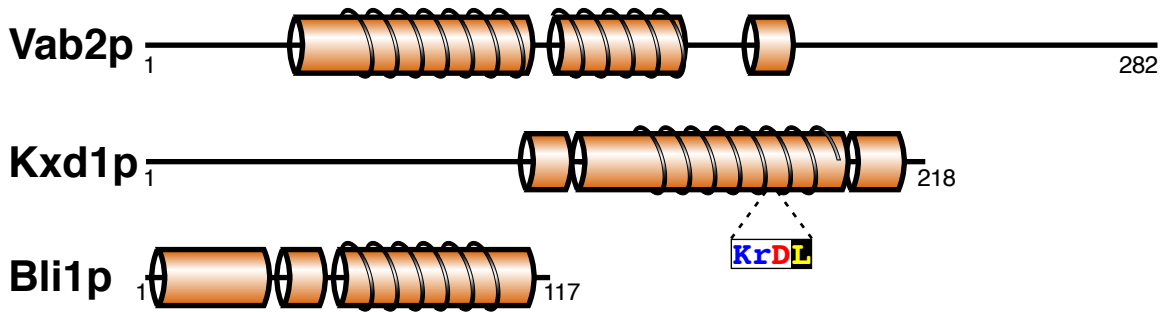


Figure 4

A



B



Supplementary Data for Hayes et al.

Consists of Tables S1 to S4, Figure S1, and supplementary references.

Table S1. Psi-BLAST results with BLOC-1 sub-units.

Blos1

NP_001478.1 (*H. sapiens*) – iteration 3 (132 hits, converged)

Posn	sequence ref	species	score	e-value
6.	NP_001478.1	<i>Homo sapiens</i>	160	2e-38
35.	NP_725401.2	<i>Drosophila melanogaster</i>	138	1e-31
43.	NP_499262.1	<i>Caenorhabditis elegans</i>	135	7e-31
54.	NP_180592.1	<i>Arabidopsis thaliana</i>	131	8e-30
130.	XP_500764.2	<i>Yarrowia lipolytica</i>	68.4	1e-10
141.	XP_451660.1	<i>Kluyveromyces lactis</i>	38.7	0.092

XP_451660.1 (*K. lactis*, see above) – iteration 2 (7 hits, converged)

Posn	sequence ref	species	score	e-value
1.	XP_451660.1	<i>Kluyveromyces lactis</i>	134	1e-30
2.	XP_002553358.1	<i>Lachancea thermotolerans</i>	129	4e-29
3.	NP_013512.1 (YLR408Cp)	<i>Saccharomyces cerevisiae</i>	118	7e-26
4.	XP_449775.1	<i>Candida glabrata</i>	117	1e-25
5.	XP_001646567.1	<i>Vanderwaltozyma polyspora</i>	112	4e-24
6.	XP_002495505.1	<i>Zygosaccharomyces rouxii</i>	112	4e-24
7.	NP_984939.1	<i>Ashbya gossypii</i>	103	2e-21
16.	ACO52029.1	<i>Rana catesbeiana</i>	36.2	0.47
34.	XP_500764.2	<i>Yarrowia lipolytica</i>	33.5	3.5

NP_013512.1 (YLR408Cp, *S cerevisiae*) – iteration 4 (61 hits)

N.B. converged at iteration 8, with 145 hits

Posn	sequence ref	species	score	e-value
1.	NP_013512.1 (YLR408Cp)	<i>Saccharomyces cerevisiae</i>	154	1e-36
24.	XP_451660.1	<i>Kluyveromyces lactis</i>	99.7	4e-20
44.	XP_500764.2	<i>Yarrowia lipolytica</i>	53.5	3e-06
54.	NP_499262.1	<i>Caenorhabditis elegans</i>	45.0	0.001
62.	XP_509120.1	<i>Pan troglodytes</i>	42.7	0.005
82.	NP_001478.1	<i>Homo sapiens</i>	39.7	0.054
140.	NP_725401.2	<i>Drosophila melanogaster</i>	35.4	0.79
202.	NP_180592.1	<i>Arabidopsis thaliana</i>	3.3	6.8

Snapi

YNL086Wp iteration 4 (12 hits, converged)

Posn	sequence ref	species	score	e-value
1.	NP_014313.1 (YNL086Wp)	<i>Saccharomyces cerevisiae</i>	122	4e-27
2.	XP_452820.1	<i>Kluyveromyces lactis</i>	104	2e-21
12.	XP_002494050.1	<i>Pichia pastoris</i>	77.0	3e-13

Cno

YDR357Cp – iterations 4 (51 hits, converged)

Posn	sequence ref	species	score	e-value
2.	EDN60686.1 (YDR357Cp)	<i>Saccharomyces cerevisiae</i>	129	4e-29
31.	XP_454923.1	<i>Kluyveromyces lactis</i>	105	1e-21
46.	XP_503339.2	<i>Yarrowia lipolytica</i>	92.0	8e-18
51.	XP_389585.1	<i>Gibberella zeae</i>	82.3	6e-15

Vab2 – iteration 6 (17 hits, converged)

Posn	sequence ref	species	score	e-value
1.	NP_010911.1 (Vab2p)	<i>Saccharomyces cerevisiae</i>	266	3e-69
5.	XP_504134.1	<i>Yarrowia lipolytica</i>	165	5e-39
17.	XP_001384198.2	<i>Scheffersomyces stipitis</i>	117	2e-24

YKL061Wp (Bli1p) – iteration 2 (6 hits, converged)

Posn	sequence ref	species	score	e-value
1.	EEU07430.1 (YKL061Wp)	<i>Saccharomyces cerevisiae</i>	120	6e-26
6.	XP_448843.1	<i>Candida glabrata</i>	87.9	3e-16

YGL079Wp (Kxd1p) – iteration 5* (142 hits)

Posn	sequence ref	species	score	e-value
16.	NP_011436.1 (YGL079Wp)	<i>Saccharomyces cerevisiae</i>	142	1e-32
26.	AAQ13622.1	<i>Homo sapiens</i>	136	9e-31
64.	NP_648580.1	<i>Drosophila melanogaster</i>	125	1e-27
101.	NP_504831.1	<i>Caenorhabditis elegans</i>	101	4e-20
126.	NP_189557.2	<i>Arabidopsis thaliana</i>	84.2	4e-15

* from iteration 6, non-KxDL proteins align with $p < 0.001$

Table S2. HHpred and HHsenser results with BLOC-1 sub-units

Pair-wise comparison of profile hidden Markov models (HMMs) was carried out (HHpred, extended with HHsenser in some cases) with the indicated seed. Data shown for top hits: full length (Len), the calculated probability it shares the same structure as the seed, (Prob - which includes calculated secondary structure), the average number of false positives expected to score better than the hit (e-value - excludes secondary structure), the ranges of residues in the HMM that match for both the seed (Query) and the hit (Template), and the number of columns aligned between seed and hit HMMs (cols).

Blos1 HHpred

# Hit	Len	Prob	e-value	Query	Template	Cols
1 NP_001478.1 Blos1 (Hs)	125	100	<1e-50	1-125	1-125	125
2 NP_499262.1 Blos1 (Ce)	129	100	<1e-50	5-125	1-121	121
3 NP_180592.1 Blos1 (At)	152	100	<1e-50	2-120	34-152	119
4 NP_725401.1 Blos1 (Dm)	143	100	<1e-50	5-125	1-121	121
5 NP_013512.1 YLR408Cp (Sc)	122	96.9	0.0042	77-121	77-121	45

Blos1 → HHsenser

# Hit	Len	Prob	e-value	Query	Template	Cols
1 NP_001478.1 Blos1 (Hs)	125	100	<1e-50	1-125	1-125	125
2 NP_499262.1 Blos1 (Ce)	129	100	<1e-50	5-125	1-121	121
3 NP_180592.1 Blos1 (At)	152	100	2.8e-45	1-120	33-152	120
4 NP_725401.1 Blos1 (Dm)	143	100	3.8e-44	5-124	1-120	120
5 NP_013512.1 YLR408Cp (Sc)	122	97.5	0.00046	49-119	46-119	71

YLR408Cp HHpred

# Hit	Len	Prob	e-value	Query	Template	Cols
1 NP_013512.1 YLR408Cp (Sc)	122	100	<1e-50	1-122	1-122	122
2 NP_499262.1 Blos1 (Ce)	129	98.0	0.00013	35-121	38-117	80
3 NP_001478.1 Blos1 (Hs)	125	97.8	0.00021	48-120	51-120	70
4 NP_180592.1 Blos1 (At)	152	97.0	0.01	14-119	21-151	104
5 NP_725401.1 Blos1 (Dm)	143	96.9	0.012	36-119	39-115	77

YLR408Cp → HHsenser

# Hit	Len	Prob	e-value	Query	Template	Cols
1 NP_013512.1 YLR408Cp (Sc)	122	100	<1e-50	1-122	1-122	122
2 NP_499262.1 Blos1 (Ce)	129	100	6.8e-29	39-122	38-118	81
3 NP_001478.1 Blos1 (Hs)	125	100	1.6e-28	37-121	40-121	82
4 NP_180592.1 Blos1 (At)	152	100	4.7e-28	14-120	21-152	104
5 NP_725401.1 Blos1 (Dm)	143	99.9	2.4e-27	37-121	36-117	82

Snapin HHpred

# Hit	Len	Prob	e-value	Query	Template	Cols
1 NP_036569.1 snapin (Hs)	136	100	<1e-50	1-136	1-136	136
2 NP_722835.1 snapin (Dm)	134	100	8.7e-44	21-133	22-134	113
3 NP_500721.1 snapin (Ce)	122	100	4.1e-43	17-134	5-120	116
4 NP_178028.2 snapin (At)	138	99.9	4.7e-24	20-122	32-133	102
8 NP_014313.1 YNL086Wp (Sc)	102	95.8	0.46	30-110	21-101	81

Snapin → HHsenser

# Hit	Len	Prob	e-value	Query	Template	Cols
1 NP_036569.1 snapin (Hs)	136	100	2.2e-40	1-136	1-136	136
2 NP_722835.1 snapin (Dm)	134	100	3.9e-34	10-128	11-129	119
3 NP_500721.1 snapin (Ce)	122	100	1.4e-31	14-136	2-122	121
5 NP_178028.2 snapin (At)	138	99.8	1.1e-19	6-127	18-138	121
7 NP_014313.1 YNL086Wp (Sc)	102	97.7	0.0033	12-110	3-101	99

YLR086Wp HHpred

# Hit	Len	Prob	e-value	Query	Template	Cols
1 NP_014313.1 YNL086Wp (Sc)	102	100	<1e-50	1-102	1-102	102
2 NP_036569.1 snapin (Hs)	136	95.6	0.57	19-101	28-110	79
3 NP_500721.1 snapin (Ce)	122	95.3	1.9	20-101	17-97	81
4 NP_722835.1 snapin (Dm)	134	94.6	1.6	19-101	29-111	79

YLR086Wp → HHsenser

# Hit	Len	Prob	e-value	Query	Template	Cols
1 NP_014313.1 YNL086Wp (Sc)	102	99.9	1.6e-25	1-102	1-102	102
2 NP_036569.1 snapin (Hs)	136	97.7	0.0032	9-101	18-110	93
3 NP_722835.1 snapin (Dm)	134	97.1	0.027	21-101	31-111	81
4 NP_500721.1 snapin (Ce)	122	96.8	0.086	20-101	17-97	81

Cno (*Dictyostelium discoideum*) HHpred*

# Hit	Len	Prob	e-value	Query	Template	Cols
1 NP_060836.1 cno (Hs)	217	100	<1e-50	3-174	56-216	161
3 NP_648414.1 cno (Dm)	169	100	<1e-50	8-173	5-165	160
6 NP_495247.1 T24H7.4 (Ce)	106	96.5	0.18	12-106	8-103	94
7 NP_010644.1 YDR357Cp (Sc)	122	96.3	1.1	2-108	15-116	99

(*Breast Carcinoma Amplified Sequence-4 isoforms x3 excluded, as this human protein is so similar to cno)

Cno (*Homo sapiens*) HHpred*

# Hit	Len	Prob	e-value	Query	Template	Cols
1 NP_060836.1 cno (Hs)	217	100	<1e-50	1-217	1-217	217
3 NP_648414.1 cno (Dm)	169	100	<1e-50	61-217	5-167	156
6 NP_010644.1 YDR357Cp (Sc)	122	96.2	1.3	48-161	8-116	109
8 NP_495247.1 T24H7.4 (Ce)	106	95.9	0.64	82-159	27-103	77

T24H7.4 (*Caenorhabditis elegans*) HHpred

# Hit	Len	Prob	e-value	Query	Template	Cols
1 NP_495247.1 T24H7.4 (Ce)	106	100	<1e-50	1-106	1-106	106
2 NP_010644.1 YDR357Cp (Sc)	122	92.8	0.58	14-106	1-117	93
3 NP_648414.1 cno (Dm)	169	90.7	0.91	1-106	1-105	103
4 NP_060836.1 cno (Hs)	217	89.3	1.8	1-106	53-162	104

YDR357Cp HHpred

# Hit	Len	Prob	e-value	Query	Template	Cols
1 NP_010644.1 YDR357Cp (Sc)	122	100	<1e-50	1-122	1-122	122
2 NP_500377.1 DUF2365 (Ce)	157	97.8	0.013	6-111	42-152	104
3 NP_060092.1 DUF2365 (Hs)	223	96.7	0.23	17-109	123-220	91
4 NP_612037.1 DUF2365 (Dm)	302	95.8	0.44	16-109	202-300	92

DUF2365 (*Caenorhabditis elegans*, Y37E11B.3) HHpred

# Hit	Len	Prob	e-value	Query	Template	Cols
1 NP_500377.1 DUF2365 (Ce)	157	100	<1e-50	1-157	1-157	157
2 NP_060092.1 DUF2365 (Hs)	223	100	<1e-50	11-152	61-222	142
3 NP_612037.1 DUF2365 (Dm)	302	100	<1e-50	12-152	128-302	141
4 NP_194064.1 DUF2365 (At)	259	99.3	5.6e-11	55-127	43-115	73
5 NP_010644.1 YDR357Cp (Sc)	122	97.9	0.0062	41-151	5-110	104

Table S3. Sequences used for Blo1/snapin consensuses, and cno line-up & Tables S1/S2

The gene identifying (GI) number and species of sequences used to make consensuses and line-ups.

Blo1		Snapin (x38)		Cno / cno-like (x24 each, + length)	
<u>GI</u>	<u>Species</u>	<u>GI</u>	<u>Species</u>	<u>GI</u>	<u>Species</u>
ANIMALS/PLANTS (x35)					
113195616	Danio rerio	148228503	Xenopus laevis	118086704	Gallus gallus 214
115692166	Strongylocentrotus purpuratus	148669506	Mus musculus	149244312	Lodderomyces elongisporus 161
116057994	Ostreococcus tauri	156365612	Nematostella vectensis	156350495	Nematostella vectensis 192
118398939	Tetrahymena thermophila	156843445	Vanderwaltozyma polyspora	156846164	Vanderwaltozyma polyspora 116
123449313	Trichomonas vaginalis	157104298	Aedes aegypti	157136111	Aedes aegypti 172
148235775	Xenopus laevis	158296992	Anopheles gambiae	158294340	Anopheles gambiae 184
15227736	Arabidopsis thaliana	167537388	Monosiga brevicollis	167538428	Monosiga brevicollis 265
156391143	Nematostella vectensis	168035684	Physcomitrella	170045619	Culex quinquefasciatus 193
157118066	Aedes aegypti	170585680	Brugia malayi	171684445	Podospora anserina 172
158301499	Anopheles gambiae	17538398	Caenorhabditis elegans	17536485	Caenorhabditis elegans 106 (T24H7.4)
170044487	Culex quinquefasciatus	189239210	Tribolium castaneum	189198760	Pyrenophora tritici 140
170590036	Brugia malayi	195999888	Trichoplax adhaerens	193582437	Acyrtosiphon pisum 164
196002611	Trichoplax adhaerens	198418879	Ciona intestinalis	19526908	Mus musculus 215
198421104	Ciona intestinalis	225462195	Vitis vinifera	196003246	Trichoplax adhaerens 177
218186731	Oryza sativa Indica	226459042	Micromonas pusilla	198429992	Ciona intestinalis 175
221101349	Hydra magnipapillata	226502642	Zea mays	210075837	Yarrowia lipolytica 116
224124784	Populus trichocarpa	238882874	Candida albicans	21356449	Drosophila melanogaster 169
226459052	Micromonas pusilla	240848775	Acyrtosiphon pisum	221112508	Hydra magnipapillata 177
226484660	Schistosoma japonicum	24581212	Drosophila melanogaster	226458182	Micromonas pusilla 188
229367874	Anoploploma fimbria	254567451	Pichia pastoris	254573206	Pichia pastoris 125
240849438	Acyrtosiphon pisum	254580643	Zygosaccharomyces rouxii	254584092	Zygosaccharomyces rouxii 108
255627133	Glycine max	255633100	Glycine max	255717240	Lachancea thermotolerans 131
260800377	Branchiostoma floridae	255718239	Lachancea thermotolerans	255951050	Penicillium chrysogenum 168
281210911	Polysphondylium pallidum	256086052	Schistosoma mansoni	256727642	Nectria haematococca 158
281363363	Drosophila melanogaster	260810887	Branchiostoma floridae	258569080	Uncinocarpus reesii 167
290997912	Naegleria gruberi	262098737	Phytophthora infestans	260944060	Clavospora lusitaniae 127
291228563	Saccoglossus kowalevskii	281204356	Polysphondylium pallidum	261353299	Verticillium albo-atrum 189
300169437	Selaginella moellendorffii	290985016	Naegleria gruberi	262112084	Phytophthora infestans 151
31980697	Mus musculus	294659996	Debaryomyces hansenii	270003414	Tribolium castaneum 125
4503955	Homo sapiens	297726007	Oryza sativa Japonica	281207674	Polysphondylium pallidum 192
47220703	Tetraodon nigroviridis	300172237	Selaginella moellendorffii	290987028	Naegleria gruberi 198
66814098	Dictyostelium discoideum	3152584	Arabidopsis thaliana	294659803	Debaryomyces hansenii 124
67479027	Entamoeba histolytica	45191013	Ashbya gossypii	295666097	Paracoccidioides brasiliensis 171
71416763	Trypanosoma cruzi	50291031	Candida glabrata	296425892	Tuber melanosporum 151
91090694	Tribolium castaneum	50305719	Kluyveromyces lactis	39971113	Magnaporthe oryzae 188
FUNGI (x27)					
116199867	Chaetomium globosum	66811200	Dictyostelium discoideum	45190845	Ashbya gossypii 129
119190001	Coccidioides immitis	6912674	Homo sapiens	46135787	Gibberella zeae 180
119481547	Neosartorya fischeri	71064114	Saccharomyces cerevisiae (YNL086W)	47208563	Tetraodon nigroviridis 231
145608262	Magnaporthe oryzae			50309819	Kluyveromyces lactis 124
146422819	Meyerozyma guilliermondii			51011035	Danio rerio 236
156043473	Sclerotinia sclerotiorum			6320564	Saccharomyces cerevisiae 122 (YDR357C)
156847365	Vanderwaltozyma polyspora			66813954	Dictyostelium discoideum 262
169624786	Phaeosphaeria nodorum			67903472	Aspergillus nidulans 167
171688892	Podospora anserina			68468893	Candida albicans 158
189198860	Pyrenophora tritici			76779596	Xenopus laevis 221
210075280	Yarrowia lipolytica			85113784	Neurospora crassa 181
242819386	Talaromyces stipitatus			8922952	Homo sapiens 217
255714152	Lachancea thermotolerans			isotig09812	Patiria miniata 197
255933021	Penicillium chrysogenum				
256735382	Nectria haematococca				
258565601	Uncinocarpus reesii 1704				
260949381	Clavospora lusitaniae				
261357041	Verticillium albo-atrum				
294656654	Debaryomyces hansenii				
295675039	Paracoccidioides brasiliensis				
296417511	Tuber melanosporum Mel28				
45190685	Ashbya gossypii				
46107490	Gibberella zeae				
50303437	Kluyveromyces lactis				
67540292	Aspergillus nidulans				
68482218	Candida albicans				
85079168	Neurospora crassa				

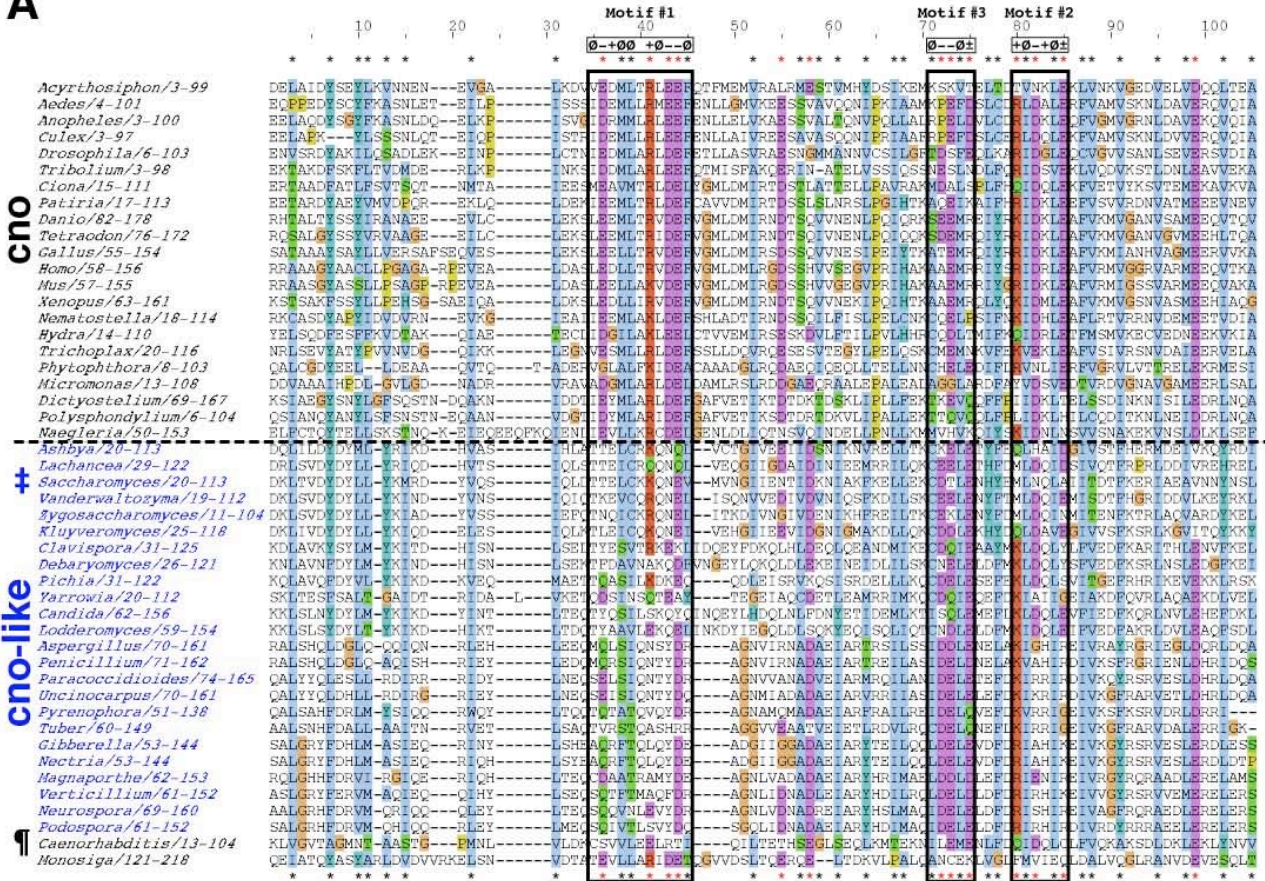
Table S4. Documented interactions within Vab2 complex

Documented interactions shown in Fig. 4 between the six components of the Vab2 complex identified by Krogan *et al.* (2006). In that paper, raw mass spectrometry data were analysed to produce a score of the probability that the interaction is genuine (= "prob"). ~7,100 core interactions scored over a threshold of $p = 0.273$. One interaction within this complex (Vab2p-Bli1p, indicated by ‡) was one of 7,000 further reactions that scored lower than the threshold – strength 0.261. Interactions that repeat one shown higher up the table are not numbered, with cross-referencing ("Xref") to the first occurrence indicated. References as indicated.

#	Bait	interactor	prob	Xref	ref
1.	Vab2p	Cnl1p	0.896		(1)
2.	Vab2p	Kxd1p	0.767		(1)
3.	Vab2p	Bls1p	0.683		(1)
4.	Vab2p	Snn1p	0.702		(1)
5.	Vab2p	Bli1	0.261‡		(1)
6.	Bls1p	Kxd1p	0.818		(1)
7.	Bls1p	Snn1p	0.647		(1)
8.	Cnl1p	Bli1p	0.748		(1)
9.	Bli1p	Kxd1p	0.404		(1)
10.	Bli1p	Bls1p	0.286		(1)
11.	Kxd1p	Snn1p			(2)
12.	Snn1p	Bli1p			(3)
	Snn1p	Bli1p		12	(4)
13.	Cnl1p	Kxd1p			(4)
	Vab2p	Kxd1p		2	(4)
	Vab2p	Snn1p		4	(4)
	Bli1p	Snn1p		12	(5)
	Cnl1p	Kxd1p		13	(5)

Supplementary Figures: Fig S1 (legend overleaf)

A



B

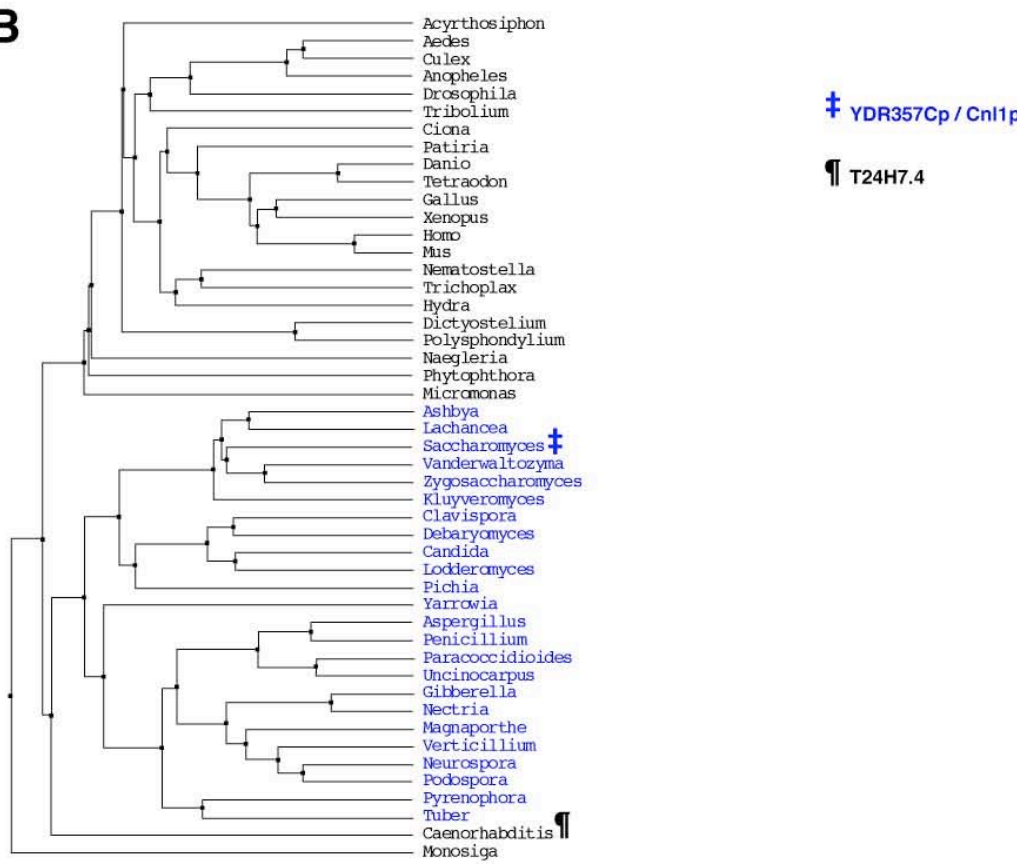


Figure S1. Relationship between cno homologues and fungal cno-like proteins.

(A). 24 cno homologues (in black, including T24H7.4[¶]) and 24 fungal cno-like homologues (in blue, including YDR357Cp/Cnl1p[‡]) were sorted in Kalign by average distance using BLOSUM62. The figure shows the region of maximal alignment across a central block of ~100 amino acids. The dotted line indicates that the two families separated almost completely (but see B). Residues at conserved positions are coloured: hydrophobic (blue), negatively charged (purple), positively charged (red), hydrophilic (T/S/N/Q: green), and tyrosine and histidine (turquoise). Also coloured are all prolines (yellow) and glycines (pink). Highly conserved positions are also indicated by asterisks (above and below, black if hydrophobic, red if charged). In addition, each of the three proposed motifs corresponding to those in Fig. 3 (Motifs #1 and #2 identified in cno⁽⁶⁾, and Motif #3 identified in this study) are boxed, and summarized above, where “Ø” is hydrophobic, and “+” “-“ & “±” are charged positive, negative or both. Motif #1 is only poorly preserved from cno (top half) into cno-like sequences (bottom half), but Motifs #2 and #3 are well conserved across both groups of sequences.

(B). Tree of the regions shown in (A), showing species. Cno homologues in nematode[¶] and the unicellular flagellate *Monosiga* are intermediate in character between the other cno sequences and the fungal cno-like family, indicating that the two main groups of sequences might have derived from a single ancestor. Sequences are listed in Table S3.

Supplementary References:

1. Krogan, NJ, et al. Global landscape of protein complexes in the yeast *Saccharomyces cerevisiae*. *Nature* 2006; 440:637-43.
2. Chin, CH, SH Chen, CW Ho, MT Ko, and CY Lin. A hub-attachment based method to detect functional modules from confidence-scored protein interactions and expression profiles. *BMC Bioinformatics* 2010; 11 Suppl 1:S25.
3. Uetz, P, et al. A comprehensive analysis of protein-protein interactions in *Saccharomyces cerevisiae*. *Nature* 2000; 403:623-7.
4. Ito, T, T Chiba, R Ozawa, M Yoshida, M Hattori, and Y Sakaki. A comprehensive two-hybrid analysis to explore the yeast protein interactome. *Proc Natl Acad Sci U S A* 2001; 98:4569-74.
5. Yu, H, et al. High-quality binary protein interaction map of the yeast interactome network. *Science* 2008; 322:104-10.
6. Cheli, VT and EC Dell'Angelica. Early origin of genes encoding subunits of biogenesis of lysosome-related organelles complex-1, -2 and -3. *Traffic* 2010; 11:579-86.